Research Article | Vol. 9, No. 2 | 1 Feb 2018 | BIOMEDICAL OPTICS EXPRESS 581
Biomedical Optics EXPRESS

In vivo imaging-guided microsurgery based on femtosecond laser produced new fluorescent compounds in biological tissues

QIQI SUN,[1,5] ZHONGYA QIN,[1,5] WANJIE WU,[1] YUE LIN,[2] CONGPING CHEN,[1] SICONG HE,[1] XUESONG LI,[1] ZHENGUO WU,[3,4] YI LUO,[2] AND JIANAN Y. QU[1,4,*]

[1]*Department of Electronic and Computer Engineering, Hong Kong University of Science and Technology, Clear Water Bay, Kowloon, Hong Kong SAR, China*
[2]*Bio-X Division, Hefei National Laboratory for Physical Science at the Microscale, University of Science and Technology of China, Hefei, Anhui, China*
[3]*Division of Life Science, Hong Kong University of Science and Technology, Clear Water Bay, Kowloon, Hong Kong SAR, China*
[4]*Center of Systems Biology and Human Health, School of Science and Institute for Advanced Study, Hong Kong University of Science and Technology, Clear Water Bay, Kowloon, Hong Kong SAR, China*
[5]*These authors contributed equally to this work*
**eequ@ust.hk*

Abstract: Femtosecond laser microsurgery has become an advanced method for clinical procedures and biological research. The tissue treated by femtosecond laser can become highly fluorescent, indicating the formation of new fluorescent compounds that can naturally label the treated tissue site. We systematically characterized the fluorescence signals produced by femtosecond laser ablation in biological tissues *in vivo*. Our findings showed that they possess unique fluorescence properties and can be clearly differentiated from endogenous signals and major fluorescent proteins. We further demonstrated that the new fluorescent compounds can be used as *in vivo* labelling agent for biological imaging and guided laser microsurgery.

OCIS codes: (300.2530) Fluorescence, laser-induced; (170.3880) Medical and biological imaging; (180.4315) Nonlinear microscopy; (300.6500) Spectroscopy, time-resolved.

References and links

1. E. E. Hoover and J. A. Squier, "Advances in multiphoton microscopy technology," Nat. Photonics **7**(2), 93–101 (2013).
2. F. Helmchen and W. Denk, "Deep tissue two-photon microscopy," Nat. Methods **2**(12), 932–940 (2005).
3. B.-G. Wang, I. Riemann, H. Schubert, K.-J. Halbhuber, and K. Koenig, "In-vivo intratissue ablation by nanojoule near-infrared femtosecond laser pulses," Cell Tissue Res. **328**(3), 515–520 (2007).
4. K. König, I. Riemann, and W. Fritzsche, "Nanodissection of human chromosomes with near-infrared femtosecond laser pulses," Opt. Lett. **26**(11), 819–821 (2001).
5. B.-G. Wang and K.-J. Halbhuber, "Corneal multiphoton microscopy and intratissue optical nanosurgery by nanojoule femtosecond near-infrared pulsed lasers," Ann. Anat. **188**(5), 395–409 (2006).
6. S. Zhuo, J. Chen, G. Wu, X. Zhu, X. Jiang, and S. Xie, "Label-free multiphoton imaging and photoablation of preinvasive cancer cells," Appl. Phys. Lett. **100**(2), 023703 (2012).
7. W. Supatto, D. Débarre, B. Moulia, E. Brouzés, J. L. Martin, E. Farge, and E. Beaurepaire, "In vivo modulation of morphogenetic movements in Drosophila embryos with femtosecond laser pulses," Proc. Natl. Acad. Sci. U.S.A. **102**(4), 1047–1052 (2005).
8. I. Maxwell, "Application of femtosecond lasers for subcellular nanosurgery," PhD Thesis (2006).
9. P. S. Tsai and D. Kleinfeld, "In Vivo Two-Photon Laser Scanning Microscopy with Concurrent Plasma-Mediated Ablation Principles and Hardware Realization," in R. D. Frostig, ed., 2nd ed., In Vivo Optical Imaging of Brain Function (Taylor & Francis Group, LLC, 2009).
10. K. Koenig, O. Krauss, and I. Riemann, "Intratissue surgery with 80 MHz nanojoule femtosecond laser pulses in the near infrared," Opt. Express **10**(3), 171–176 (2002).
11. J. A. Galbraith and M. Terasaki, "Controlled damage in thick specimens by multiphoton excitation," Mol. Biol. Cell **14**(5), 1808–1817 (2003).

Biomedical Optics EXPRESS

12. A. K. N. Thayil, A. Pereira, M. Mathew, D. Artigas, E. M. Blanco, and P. Loza-Alvarez, "Decrease in laser ablation threshold for epithelial tissue microsurgery in a living Drosophila embryo during dorsal closure," J. Microsc. **232**(2), 362–368 (2008).
13. V. Hovhannisyan, W. Lo, C. Hu, S.-J. Chen, and C. Y. Dong, "Dynamics of femtosecond laser photo-modification of collagen fibers," Opt. Express **16**(11), 7958–7968 (2008).
14. R. Milo, "What is the total number of protein molecules per cell volume? A call to rethink some published values," BioEssays **35**(12), 1050–1055 (2013).
15. J. E. P. Jr and M. T. Murray, *Textbook of Natural Medicine* (Elsevier Health Sciences, 2012).
16. D. Li, W. Zheng, and J. Y. Qu, "Time-resolved spectroscopic imaging reveals the fundamentals of cellular NADH fluorescence," Opt. Lett. **33**(20), 2365–2367 (2008).
17. S. Zhu, J. Zhang, L. Wang, Y. Song, G. Zhang, H. Wang, and B. Yang, "A general route to make non-conjugated linear polymers luminescent," Chem. Commun. (Camb.) **48**(88), 10889–10891 (2012).
18. M. Drobizhev, N. S. Makarov, S. E. Tillo, T. E. Hughes, and A. Rebane, "Two-photon absorption properties of fluorescent proteins," Nat. Methods **8**(5), 393–399 (2011).
19. A. Vogel, J. Noack, G. Hüttman, and G. Paltauf, "Mechanisms of femtosecond laser nanosurgery of cells and tissues," Appl. Phys. B **81**(8), 1015–1047 (2005).
20. C. B. Schaffer, J. F. García, and E. Mazur, "Bulk heating of transparent materials using a high-repetition-rate femtosecond laser," Appl. Phys. Mater. Sci. Process. **76**(3), 351–354 (2003).
21. M. J. Farrar, I. M. Bernstein, D. H. Schlafer, T. A. Cleland, J. R. Fetcho, and C. B. Schaffer, "Chronic in vivo imaging in the mouse spinal cord using an implanted chamber," Nat. Methods **9**(3), 297–302 (2012).
22. G. Yang, F. Pan, C. N. Parkhurst, J. Grutzendler, and W.-B. Gan, "Thinned-skull cranial window technique for long-term imaging of the cortex in live mice," Nat. Protoc. **5**(2), 201–208 (2010).
23. D. Davalos, J. Grutzendler, G. Yang, J. V. Kim, Y. Zuo, S. Jung, D. R. Littman, M. L. Dustin, and W.-B. Gan, "ATP mediates rapid microglial response to local brain injury in vivo," Nat. Neurosci. **8**(6), 752–758 (2005).
24. Q. Yang, L. Wei, X. Zheng, and L. Xiao, "Single Particle Dynamic Imaging and Fe3+ Sensing with Bright Carbon Dots Derived from Bovine Serum Albumin Proteins," Sci. Rep. **5**(1), 17727 (2015).
25. X. Wang, K. Qu, B. Xu, J. Ren, and X. Qu, "Microwave assisted one-step green synthesis of cell-permeable multicolor photoluminescent carbon dots without surface passivation reagents," J. Mater. Chem. **21**(8), 2445 (2011).

1. Introduction

Femtosecond lasers used in multiphoton nonlinear optical microscopy have become indispensable tools for biological research [1]. In multiphoton microscopy, two or more photon absorption process is effectively restricted to the focal volume, which provides intrinsic three-dimensional optical sectioning capability [2]. Due to the highly localized nonlinear absorption process, femtosecond lasers are also utilized in laser surgery to precisely cut and/or remove the targeted cells or tissue *in vivo* [3]. As a promising light source for surgery, femtosecond lasers with a MHz repetition rate have been successfully demonstrated to slice through chromosomes [4], cut the cornea in intraocular refractive surgery [5], ablate pre-invasive cancer cells in epithelial tissue [6], modulate the morphogenetic movements in *Drosophila* embryos [7], and many other applications [8,9]. Therefore, a femtosecond laser can potentially serve as the light source for both multiphoton microscopy and laser surgery simultaneously to achieve microscopic imaging-guided surgery [9]. Interestingly, previous studies have reported that the laser surgery site becomes highly fluorescent after laser ablation [6,7,9–12]. Although these fluorescent compounds produced during laser surgery could be used as natural labeling agents for *in vivo* biological imaging and guided laser microsurgery, little studies have been conducted on characterizing the fluorescence properties and understanding their formation mechanism.

Since new fluorescence emissions during laser surgery have been observed in a variety of biological tissues, such as brain tissue of rats [9], porcine cornea [10], epithelial tissue of *Drosophila* embryos [12] and bovine tendon collagen [13], the laser produced fluorescent compounds likely originate from a common substance in the different tissues. Protein is the most abundant compound in animals except water, accounting for approximately half of the total dry mass [14,15]. Therefore, protein could be the source material that forms fluorescent compounds through laser ablation. In this work, we aim to comprehensively characterize the femtosecond laser produced fluorescence in biological tissues and explore their applications. We first developed a combined single-photon confocal and two-photon fluorescence spectroscopy system that records time- and spectral-resolved single- and two-photon

Biomedical Optics EXPRESS

fluorescence emissions at the same location of sample. Using this system, we systematically characterized the fluorescence properties of femtosecond laser treated biological samples. The unique properties of the new fluorescence served as a basic guide for efficiently differentiating the femtosecond laser treated tissue from surrounding intact tissue through the single-photon confocal or two-photon microscopy. In addition, we characterized the femtosecond laser produced fluorescence from albumin, a commonly used protein in biological research, and compared the properties of new fluorescence in albumin and biological tissues. Finally, we demonstrated applications of *in vivo* imaging-guided microsurgery in muscle and neuroscience research.

2. Method and materials

2.1 Single- and two-photon excited fluorescence spectroscopy imaging system

We built an optical spectroscopy imaging system to study the spectral and temporal properties of the fluorescent compounds produced through laser ablation in biological tissue. A system schematic is shown in Fig. 1. Briefly, a femtosecond Ti:Sapphire laser (Mira900-S, Coherent) of wavelength tuning range from 740 nm to 880 nm and its second harmonic generation (SHG) from a β-barium borate crystal (BBO) of wavelength range from 370 nm to 440 nm were used as the light sources for two-photon and single-photon excitations, respectively. The femtosecond laser and its SHG beam were combined using a dichroic mirror and switched alternatively to excite two- and single-photon fluorescence signals from sample sequentially. The combined beams passed through a pair of galvo mirrors for x-y lateral scanning and a water immersion objective (UAPON 40XW340, 1.15 NA, Olympus) was driven by an actuator (Z625B, Thorlabs) for axial sectioning. Using this setup, we studied the single- and two-photon signals excited at the same location in a sample. The backward fluorescence signals via both single- or two-photon excitation were directed to the detection channel by a 50/50 beamsplitter (BSW10R, Thorlabs) and recorded in a descanned configuration. A 200 mm focal length doublet lens was used to focus the fluorescence signal into a fiber of 100 μm core diameter, which acted as a pinhole in the confocal detection of single-photon excited fluorescence from the samples. The filter set included a shortpass filter (ET700sp, Chroma) to reject the near-infrared two-photon excitation laser, and a set of longpass filters to filter out the single-photon excitation laser. The cut-off wavelength of each long pass filter was approximately 30 nm to 50 nm longer than the single-photon excitation wavelength. The fluorescence signals conducted by the fiber were passed through a spectrograph equipped with a 16 photomultiplier tube (PMT) array and a time-correlated single photon counting (TCSPC) module (PML-16-0 and SPC-150, Becker & Hickl). The system recorded signals of wavelengths ranging from 403 nm to 598 nm with a 13 nm spectral resolution and about 200 ps temporal resolution. The axial and lateral resolutions were approximately 3.5 μm and 0.5 μm for confocal detection of single-photon signals, and 1.2 μm and 0.4 μm for two-photon signals, respectively. The wavelength and intensity response of this spectroscopy imaging system were calibrated using a mercury and halogen lamp (DH2000, Ocean Optics), respectively. The fluorescence decay curve was fitted using the software SPCImage (Becker & Hickl) with an incomplete decay dual exponential function model. The emitted light of wavelengths ranging from 481 nm to 507 nm and from 507 nm to 533 nm was used for single- and two-photon excited fluorescence lifetime fitting, respectively.

To ablate biological sample and generate the new fluorescent compounds, a 740 nm femtosecond laser of 150 mW was first focused at a fixed point in a sample for 1~5 seconds. In the study of properties of new fluorescence compounds, the excitations of wavelength ranging from 370 nm to 440 nm and from 740 nm to 880 nm were used to excite the single- and two-photon fluorescence, respectively. To avoid possible photobleaching, the laser power for single- and two-photon excitation was less than 20 μW and 20 mW, respectively. The spectroscopic images for studying properties of laser produced fluorescent compounds had 100 μm × 100 μm field of view, and the acquisition time of each image was 4~8 seconds. To

Biomedical Optics EXPRESS

eliminate the interference of autofluorescence from the intact areas, the fluorescence properties were extracted only from the laser ablated areas using an imaging-guided spectroscopy method that was described in our previous study [16]. As an example, *in vivo* measurements of new fluorescence signals from ablated skin tissue of mouse are shown in Fig. 2. Since laser produced fluorescent compounds exhibit much stronger fluorescence emission than the endogenous fluorophores as shown in Fig. 2(c), we can easily extract the laser ablated region by applying an intensity threshold.

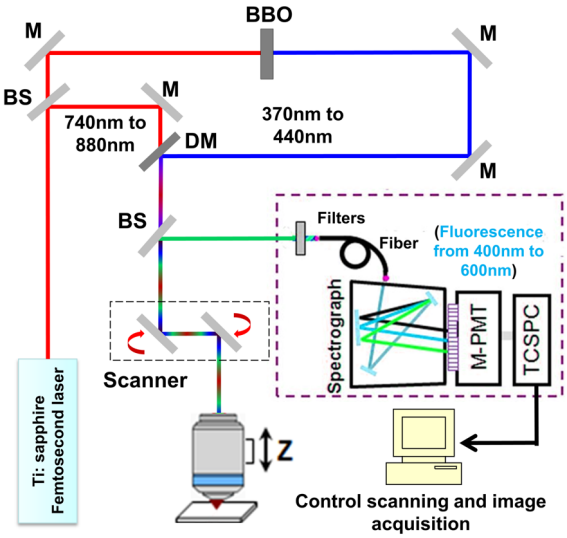

Fig. 1. Schematic of single- and two-photon fluorescence spectroscopy imaging system. M: mirror; BS: 50/50 beam splitter; DM: dichroic mirror; BBO: Beta Barium Borate crystal; M-PMT: 16 channels photomultiplier tube array; TCSPC: time-correlated single photon counting.

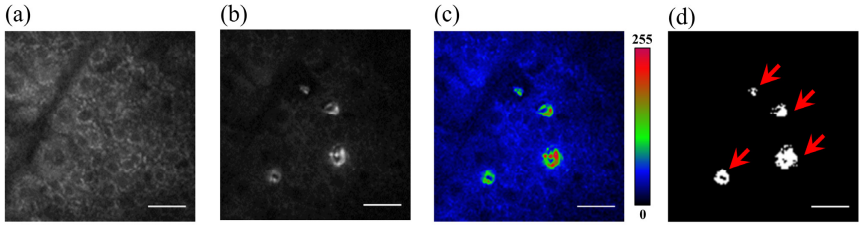

Fig. 2. Imaging-guided fluorescence spectroscopy in biological tissue *in vivo* (740 nm excitation and 400-600 nm detection). (a) Fluorescence image of mouse ear skin tissue before laser ablation; (b) fluorescence image after laser ablation; (c) color-coded fluorescence intensity image (8-bit) after laser ablation, and (d) binary mask for extraction of signals from laser produced fluorescent compounds in tissue (red arrows indicate laser ablation sites). Scale bar: 20 μm.

2.2 Sample preparation

In this work, we characterized the properties of laser produced fluorescence from three representative tissues (skin, muscle and brain) of distinct morphological structures and biochemical compositions. The skin and muscle tissues were studied in live mice and brain tissues were freshly excised from mice. Specifically, the ear skin, tibialis anterior muscle and brain neocortex tissues from ICR and C57BL/6J mice were used as representative biological tissues. To study the properties of femtosecond laser produced fluorescent compounds in skin *in vivo*, the ear skin with hair removed using depilatory lotions (Veet®) was directly exposed to the spectroscopy imaging system (Fig. 1) for ablation and spectroscopy measurements. In the study of muscle tissue *in vivo*, the skin of mouse leg was surgically removed to expose the

Biomedical Optics EXPRESS

tibialis anterior muscle to the same spectroscopy imaging system. The mice were anesthetized via inhalation of isoflurane throughout all the experiments. The brain neocortex tissues were freshly isolated from the mice and immediately put under the spectroscopy imaging system for laser ablation and fluorescence characterization. All the experimental procedures were approved by University Institutional Animal Care committees and conform to NIH guidelines. To prepare the protein sample, albumin (A7906, Sigma) was first dissolved in Milli-Q water at a concentration of 0.2 g/ml. The laser ablation and fluorescence characterization in albumin sample were performed using the same system shown in Fig. 1. Finally, *CX3CR1-GFP* mouse line with microglia labelled by GFP and *Thy1-EGFP* transgenic mouse line with neurons and axons labelled by EGFP were used to demonstrate *in vivo* imaging-guided microsurgery for neuroscience research.

2.3 Two-photon microscope system for in vivo applications

To demonstrate the applications of the laser produced fluorescent compounds, we built a two-photon fluorescence lifetime microscope with non-descanned detection configuration. Specifically, the emission signals collected by the objective were immediately reflected to the detection system using a dichroic mirror (FF705-Di01, Semrock). A dichroic mirror at 488 nm (Di02-R488, Semrock) or 550 nm (550DCLP, Chroma), chosen according to the requirements of *in vivo* imaging in different tissues, separated the signals into a short- and long-wavelength channel. Appropriate filters were placed in front of the detectors to reject the excitation laser and select particular wavelength ranges of detection. Signals were recorded using two sensitive GaAsP hybrid PMT detectors (HPM-100-40, Becker & Hickl), respectively, and analyzed by a TCSPC module with router (SPC-150, Becker & Hickl). To simplify the *in vivo* microsurgery procedure, we used the femtosecond laser at the same wavelength (920 nm) for the ablation and imaging of biological tissues. The laser power for ablation and two-photon fluorescence imaging were 100~300 mW and 20~60 mW, respectively. The time for laser ablation and image acquisition were 1~5 seconds and 4~8 seconds, respectively.

3. Results and discussions

3.1 Characterization of new fluorescence in laser ablated biological samples

The properties of femtosecond laser produced fluorescence in biological tissues (skin, muscle and brain) were systematically characterized via single- and two-photon excitation at different excitation wavelengths. The representative results with ablation laser at 740 nm are summarized in Fig. 3(a)-3(c). As can be seen, the peak of the fluorescence emission spectra via single-photon excitation shifts from blue to red with the increase of the excitation wavelength. These excitation wavelength-dependent fluorescence emission could be attributed to that the chemical reactions induced by laser ablation process generate complex fluorescent compounds of multiple fluorescent centers, each of which is efficiently excited by a certain wavelength [17]. However, all two-photon excited fluorescence emission spectra show peaks at wavelengths longer than 500 nm, even for short-wavelength excitation (e.g., 740 nm). This phenomenon may arise from a well-studied resonance enhancement effect [18], by which the red fluorescence emission intensity is greatly increased because the short excitation wavelengths are near resonant to the emission wavelength of red fluorescent centers. Therefore, the 370 nm light is favorable for exciting blue emission fluorescent centers via single-photon process, while 740 nm light excites both blue and red fluorescence via two-photon process. This results in the large discrepancy between single- and two-photon excited fluorescence emission spectra, especially for short-wavelength excitations. The properties of new fluorescence emission are unique and significantly different from the tissue autofluorescence and fluorescent proteins. In the biomedical applications, these measured fluorescence emission spectra can serve as a basic guide for efficiently detecting and imaging

Biomedical Optics EXPRESS

the femtosecond laser treated tissue areas through the single-photon confocal or two-photon microscopy. Additionally, the fluorescence lifetimes, another important fluorescence property of these femtosecond laser produced fluorescent compounds were found to be approximately 1 ns in all biological tissues, shorter than the widely used fluorescent proteins such as enhanced green fluorescence protein (EGFP) (3.43 ns) and tdTomato (3.6 ns) [18]. Therefore, these newly produced fluorescence can be also clearly imaged and distinguished from the fluorescent proteins with a standard fluorescence lifetime imaging microscopy (FLIM). Finally, it should be emphasized that the fluorescence properties are not determined by the wavelength of ablation femtosecond laser. We found that the spectral and temporal characteristics of the new fluorescence produced by the ablation laser of wavelength from 740 to 920 nm are similar.

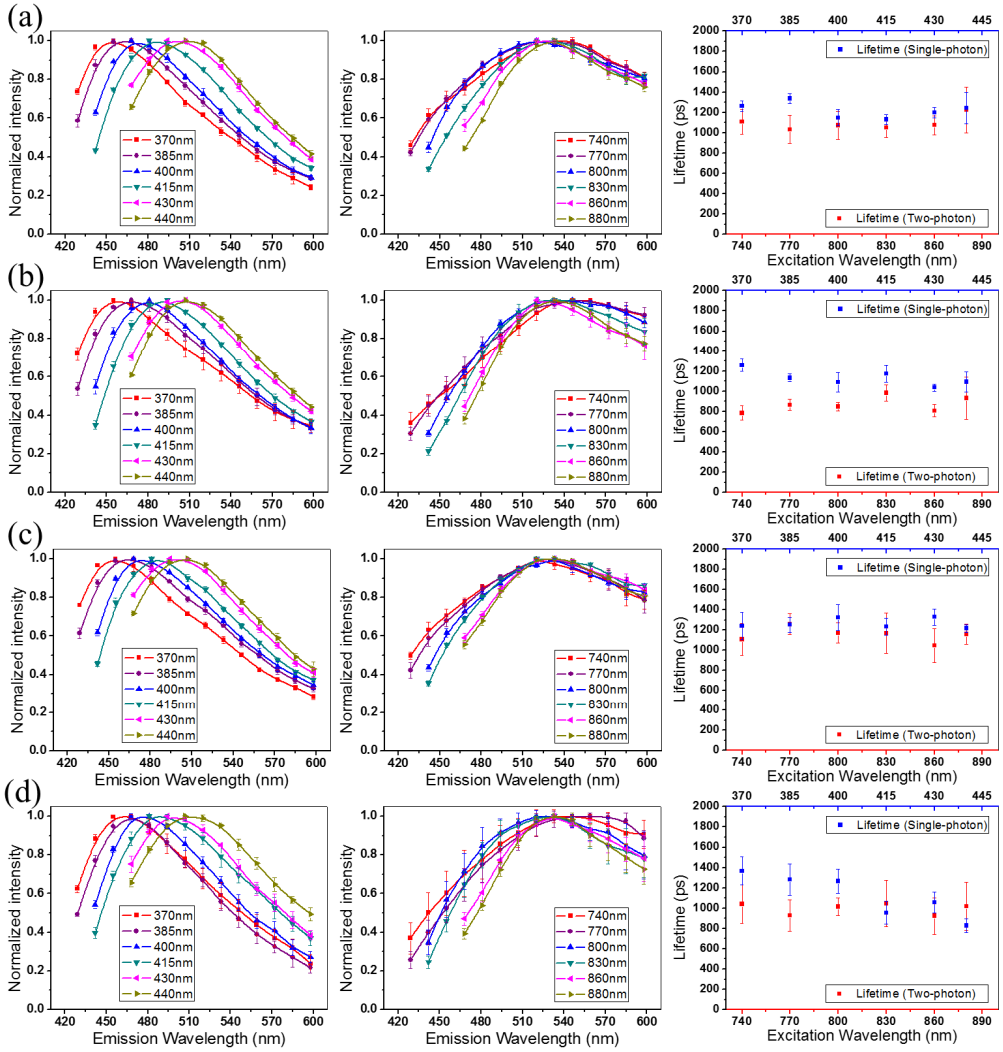

Fig. 3. Spectral and temporal properties of femtosecond laser produced fluorescent compounds in (a) mouse skin, (b) muscle, (c) brain tissue and (d) albumin. Left column: single-photon excited (370 nm to 440 nm) fluorescence emission spectra; middle column: two-photon excited (740 nm to 880 nm) fluorescence emission spectra; right column: single- and two-photon excited fluorescence lifetimes. Each fluorescence spectrum and lifetime were obtained based on the integration of fluorescence over the ablated site. Error bars represent ± SD of three measurements.

Biomedical Optics EXPRESS

As shown in Fig. 3(a)-3(c), similar fluorescence emission spectra and lifetimes are observed among different tissues under the same excitation conditions, indicating that the newly produced fluorescent compounds are alike in all of these tissues. Here, we hypothesize that the fluorescent compounds may originate from the interaction of femtosecond laser with proteins that are abundant and ubiquitous in the biological tissues. To address the hypothesis, we conducted the same laser ablation experiments on albumin samples. We characterized the properties of new fluorescence in the ablated albumin and the results are shown in Fig. 3(d). Similarly, the peak of the single-photon excited fluorescence emission spectra is dependent on the excitation wavelength, and the two-photon excited fluorescence emission spectra are different from those obtained by single-photon excitation. The lifetime is also approximately 1 ns, consistent with the results in biological tissues. The similarity suggests that the fluorescent compounds in tissue may be from the interaction between laser and proteins.

Previous study indicated that long-pulsed or cw laser ablation is believed to rely on the local thermolysis and formation of vapor bubbles via single-photon absorption process, which highly depends on the absorption properties of treated biological samples [19]. However, the tissue ablation by a femtosecond laser with high peak power and repetition rate (~80 MHz) is achieved by the accumulative chemical effect(s) via multiphoton ionization and plasma-mediated absorption [19]. In general, the average power used in quasi-cw laser surgery is considerably higher than that in femtosecond laser surgery [19]. In this work, we studied the ablation with cw output from the Ti:sapphire femtosecond laser system when its mode locking was turned off. It was found that even at the highest power of cw laser on the tissue samples (~300 mW) there was neither ablation nor fluorescence emission detected in the biological samples after 4 seconds illumination. The result was consistent with other groups' work and indicated that the tissue ablation and production of new fluorescent compounds should originate from the nonlinear absorption effect induced by the femtosecond laser pulse of high peak power [11,19]. Finally, it should be pointed out that the heat accumulation in the laser ablation region may also play a role in the production of new fluorescent compounds since the pulse interval of a standard Ti:sapphire femtosecond laser with 80 MHz repetition rate is shorter than the heat diffusion time [8,20]. Therefore, the new fluorescent compounds may originate from the photochemical or photothermal process based on the multiphoton absorption of femtosecond laser in the biological tissue.

3.2 In vivo imaging-guided microsurgery

The new fluorescent compounds produced through femtosecond laser ablation have unique spectral and temporal properties that can be used to label the ablated tissue for a variety of applications. To demonstrate that the femtosecond laser produced fluorescence can be used for *in vivo* label-free imaging and guided microsurgery, we first performed the laser surgery and two-photon microscopy in muscle tissue of live wild-type mice. In the experiment, the leg muscle of an anesthetized mouse was surgically exposed for laser microsurgery and two-photon microscopy using the femtosecond laser of same wavelength at 920 nm. A dichroic mirror at 488 nm (Di02-R488, Semrock) was used to separate SHG and laser produced fluorescence into two detection channels. Using the new fluorescence signals as feedback to precisely control the ablation laser, fine laser cuttings with low ablation power were achieved at different depths. As shown in Fig. 4(a)-4(b), the laser produced fluorescence from the cutting sites (red-colored) and SHG from sarcomeres of intact muscle (green-colored) can be clearly differentiated in the spectral domain. The cutting trace was strictly confined in a small three-dimensional volume and did not cause damage to surrounding structures in the muscle fibers. This can be confirmed by the SHG signals of myosin in sarcomeres showing that all adjacent sarcomeres remained intact after laser microsurgery. With increasing the power of laser ablation, we created a large-size laser cutting in muscle to visualize the dynamic process of muscle fiber degeneration (Fig. 4(c) and Visualization 1). Moreover, the new fluorescence signal can also be clearly differentiated from SHG signal in the time domain as shown in Fig.

Biomedical Optics EXPRESS

4(d)-4(f) and Visualization 2. The lifetime-coded images are nearly identical to the spectral-coded images. The results demonstrate that the laser produced fluorescence in tissue can be used in the label-free imaging to guide and evaluate the laser microsurgery *in vivo*.

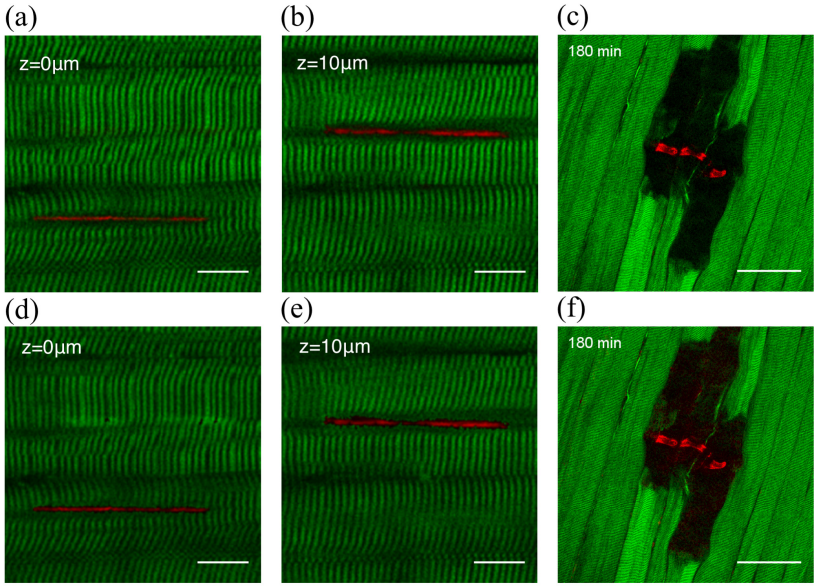

Fig. 4. *In vivo* application of femtosecond laser produced fluorescence in label-free imaging-guided microsurgery in mouse muscle. (a-c) Spectral-coded images of fine laser cutting in muscle fibers at two depths separated by 10 μm (a-b) and cutting of three muscle fibers (c). The SHG signal of myosin detected at 447 nm channel is colored in green and the laser produced fluorescence detected at 525 nm channel is colored in red; (d-f) corresponding lifetime-coded images. The SHG signal of myosin (short lifetime) is colored in green and the laser produced fluorescence (long lifetime) is colored in red. Scale bar: (a-b, d-e) 20 μm, (c, f) 100 μm.

Laser axotomy is a neurosurgery technique based on highly localized femtosecond laser ablation. It allows for precise dissection of single axon. Next, we demonstrate that the femtosecond laser produced fluorescence can be used to precisely image the location of dissection and evaluate the degree of damage in the laser lesion site. In this work, we implanted a spinal chamber for chronic imaging to mouse (Fig. 5(a)-5(c)) [21]. This imaging window enabled performing the laser axotomy and two-photon microscopy in the spinal cord of live mouse. First, the spinal cord of live *Thy1-EGFP* mouse was imaged through the chronic implanted chamber for the selection of targeted axons. Then, we implemented two laser axotomy at low and high power levels of femtosecond laser at 920 nm to dissect the targeted axons with small and large damage, respectively. The two-photon microscopy using the same femtosecond laser was performed following the axotomy procedure and the results are shown in Fig. 5(d)-5(g). Here, a dichroic mirror at 550 nm (550DCLP, Chroma) was used to separate GFP and the new fluorescence signal. The axons labelled by GFP are colored in green and the ablation laser produced fluorescence from the dissected sites are colored in red. As shown in the two-photon images (Fig. 5(d)-5(e)), the signals of laser produced fluorescent compounds clearly indicate the laser ablated sites. In addition, the new fluorescent region of ablated tissue provides accurate information to evaluate the damage caused by the axotomy procedure at different laser power levels. It should also be emphasized that the laser produced fluorescence can also be differentiated from the signals of major fluorescent proteins in time domain because of its much shorter lifetime. As shown in Fig. 5(f)-5(g), the lesions can be identified as clearly as the results shown in Fig. 5(d)-5(e) by using FLIM mode of our two-photon fluorescence microscope system.

Biomedical Optics EXPRESS

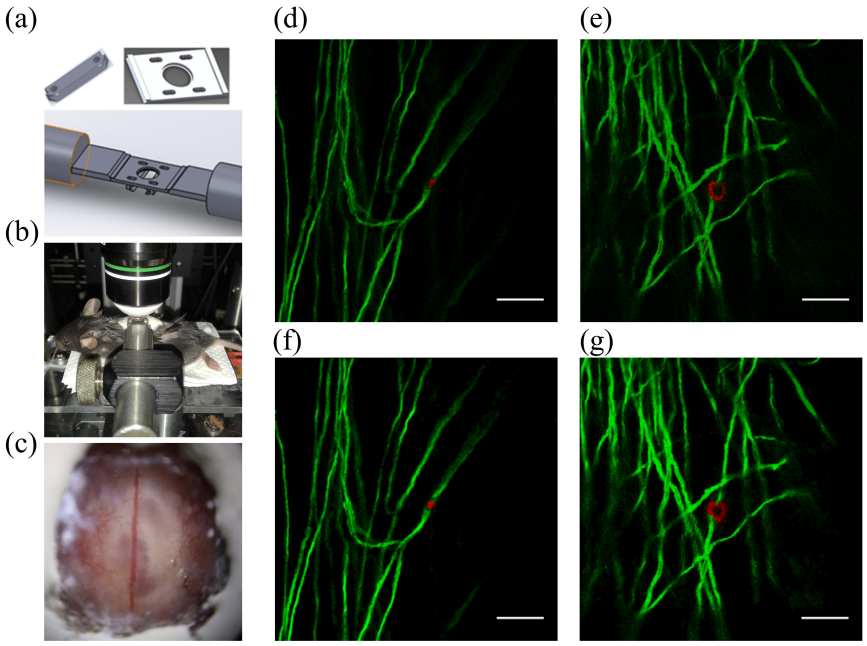

Fig. 5. Application of femtosecond laser produced fluorescence in laser axotomy. (a) Home-made spinal chamber; (b) mouse mounting scheme for *in vivo* imaging of spinal cord; (c) bright field image through the spinal cord window; (d-e) spectral-coded two-photon images of laser axotomy in mouse spinal cord with small damage (d) and large damage (e). Green: signals from GFP labelled spinal cord detected at 525 nm channel, red: signals from laser ablation site detected at 593 nm channel; (f-g) corresponding lifetime-coded images. Green: lifetime of > 1.4 ns, red: lifetime of < 1.4 ns. Scale bar in (d-g): 50 μm.

Finally, we demonstrate the application of this fluorescence in the study of immune response to tissue injury in brain. A *CX3CR1-GFP* mouse cortex with GFP-labelled microglia was directly imaged through a thinned-skull cranial window technology (Fig. 6(a)-6(b)) [22]. We first inflicted an injury in the cortex through laser ablation and then imaged the ablated site and microglia simultaneously. Again, a dichroic mirror at 550 nm (550DCLP, Chroma) was used to separate GFP signal and the new fluorescence signal. As can be seen from Fig. 6(c)-6(d), the laser injury site in the center of image can be clearly differentiated from the GFP-labelled microglia in the spectral domain. The dynamic interactions between the microglia and laser injured brain tissue are illustrated in Visualization 3, showing that the microglia quickly responded to the tissue damage within six minutes. The microglial processes extended toward the injury site and completely wrapped around it within 40 minutes. Although this rapid microglial response to laser injury of brain tissue has been previously reported [23], the fluorescence from the laser injury site and the microglia were not clearly separated, making it difficult to determine when the processes reach to and wrap around the injured brain tissue.

Biomedical Optics EXPRESS

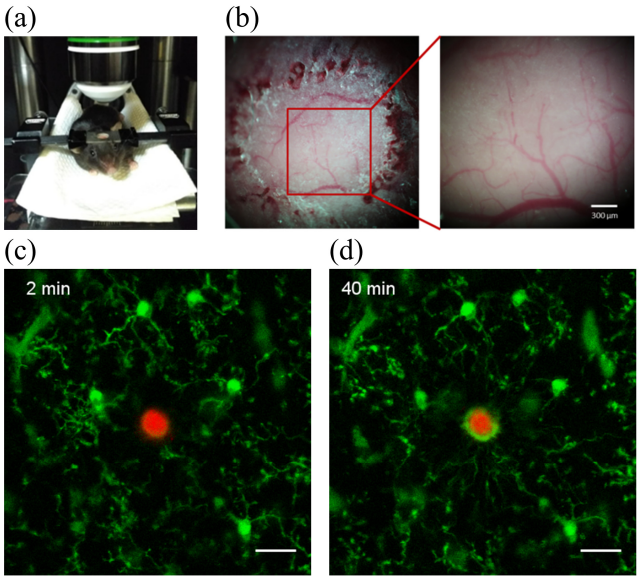

Fig. 6. Application of femtosecond laser produced fluorescence in the study of immune response to the injury in brain. (a) Mouse mounting scheme for brain imaging; (b) bright field image of thinned-skull window; (c-d) two-photon images of GFP-labelled microglia (green) and laser damaged tissue (red) in mouse brain at 2 min after injury (c) and 40 min after injury (d) (details in Visualization 3). Green: signals detected at 525 nm channel; red: signals detected at 593 nm channel. Scale bar in (c-d): 20 μm.

4. Conclusion

In this work, we characterized the laser ablation produced new fluorescent compounds in the biological tissues and demonstrated that they can be used as *in vivo* labelling agent for biological imaging and guided laser microsurgery. Importantly, this technology is based on a standard two-photon microscope system and can be easy to pursue by a wide range of laboratories in a variety of biological and clinical applications. Although our study results suggest that the fluorescent compounds may originate from the interaction of femtosecond laser and protein, detailed formation process remains unknown. Recent study reported that carbon dots are highly fluorescent and could be produced by high-temperature carbonization of proteins and other organic materials [17,24,25]. The femtosecond laser generates highly localized heating in the ablated tissue site. The ablation process could cause high temperature carbonization of tissue and produce fluorescent carbon dots. However, large-scale study and further analysis such as Raman spectroscopy and transmission electron microscopy must be conducted to reveal the structural changes of biological tissue induced by the laser ablation and to identify the fluorophore(s) of the new fluorescent compounds.

Funding

Hong Kong Research Grants Council (662513, 16103215, 16148816, T13-607/12R, T13-706/11-1, AOE/M-09/12); Hong Kong University of Science & Technology (HKUST) (RPC10EG33).

Disclosures

The authors declare that there are no conflicts of interest related to this article.